Journal of Industrial and Engineering Chemistry 73 (2019) 192–197

Contents lists available at ScienceDirect

Journal of Industrial and Engineering Chemistry

journal homepage: www.elsevier.com/locate/jiec

Synthesis of quinoxaline-based polymers with multiple electron-withdrawing groups for polymer solar cells

Shinta Lieviana Handoko[a,1], Ho Cheol Jin[b,1], Dong Ryeol Whang[c], Sella Kurnia Putri[a], Joo Hyun Kim[b,*], Dong Wook Chang[a,*]

[a] Department of Industrial Chemistry, Pukyong National University, 48513 Busan, South Korea
[b] Department of Polymer Engineering, Pukyong National University, 48513 Busan, South Korea
[c] Linz Institute for Organic Solar Cells (LIOS)/Institute of Physical Chemistry, Johannes Kepler University Linz, 4040, Linz, Austria

ARTICLE INFO

Article history:
Received 12 November 2018
Received in revised form 9 January 2019
Accepted 17 January 2019
Available online 26 January 2019

Keywords:
Quinoxaline
Electron-withdrawing
Polymer solar cell
Indacenodithiophene
Indacenodithieno[3,2-b]thiophene

ABSTRACT

Two quinoxaline-based conjugated polymers with multiple electron-withdrawing moieties were synthesized by the Stille coupling reaction for polymer solar cells (PSCs). For the construction of a typical donor-π-acceptor structure, the electron-donating indacenodithiophene (IDT) and indacenodithieno [3,2-b]thiophene (IDTT) were linked to the electron-withdrawing quinoxaline ($DPQCF_3F$) that contained trifluoromethyl and fluorine units via a thiophene bridge to produce **PIDT-Qx** and **PIDTT-Qx**, respectively. Owing to the significant contribution of the $DPQCF_3F$ unit in the polymer backbone, V_{oc} of the inverted-type PSCs was increased up to 0.92 V. In addition, the replacement of two thiophenes of IDT to two thieno [3,2-b] thiophene units of IDTT in the quinoxaline-based polymer backbone can efficiently improved the light absorption and charge carrier mobility of the resultant polymer. Therefore, a higher PCE of 4.54% was achieved from the device based on **PIDTT-Qx** with a short circuit current density of 9.30 mA/cm^2, an open-circuit voltage of 0.92 V, and a fill factor of 53%, compared with the device based on **PIDT-Qx** (2.83%).

Introduction

In recent years, polymer solar cells (PSCs) with a bulk-heterojunction (BHJ) structure have attracted great attention, owing to their lightweight, flexibility, good cost-effectiveness, simple device architecture, and potential for the large-area fabrication [1–3]. The BHJ structure is usually created by blending of conjugated polymers and fullerene derivatives as an electron donor and an electron accepter, respectively, which results in a large interfacial area between them in the active layer of the PSC. In this BHJ condition, the charge transfers from the excited polymeric donors to the fullerene-based acceptors, and fast exciton dissociation can be promoted. Thus, energy conversion from sunlight to electricity in the PSCs is facilitated [4–6]. Previously, numerous PSCs with a BHJ structure have been developed and have shown a high power conversion efficiency (PCE) of up to 13% [7–9].

Among the diverse approaches for improving the photovoltaic performances of the PSCs, the proper molecular design of the polymeric donors is considered as one of the most important parameters. The great efforts have been focused on lowering the bandgap and modulating the energy levels of the conjugated polymers by the delicate control of the molecular architectures. In order to obtain low bandgap conjugated polymers, an alternating electron-donating and electron-accepting component to create donor-acceptor configurations has been widely utilized, because of the facile formation of the intramolecular charge transfer (ICT) state between the electron-donating and electron-accepting components [10–13]. Apart from reducing the bandgap, the introduction of electron-withdrawing substituents such as fluorine (F) [14–16], cyano (CN) [17], sulfonyl (SO_2) [18], and trifluoromethyl (CF_3) [19] units, specifically on the electron-accepting constituent of the polymer backbone, can efficiently enhance the photovoltaic performance of the PSCs by the lowering lowest occupied molecular orbital (LUMO) and highest occupied molecular orbital (HOMO) level of the conjugated polymers. A low-lying HOMO level of the polymeric donor can improve the photovoltaic properties by increasing the open-circuit voltage (V_{oc}) of the PSC [20,21].

Recently, it has been reported that the position and population of the electron-withdrawing moieties in the polymer backbone are

* Corresponding authors.
E-mail addresses: jkim@pknu.ac.kr (J.H. Kim), dwchang@pknu.ac.kr (D.W. Chang).
[1] S. L. Handoko and H. C. Jin equally contributed to this research.

https://doi.org/10.1016/j.jiec.2019.01.024
1226-086X/

of great importance to determine the performances of PSCs [22–24]. In particular, when the number of electron-withdrawing F atoms on the electron-accepting quinoxaline (Qx) unit in D-A type polymers increases, the power conversion efficiency (PCE) of the PSCs with these polymers is increased [25]. Moreover, the incorporation of the strong electron-withdrawing CF_3 moieties together with the F atoms on the alkoxy-modified electron-accepting 2,3-diphenylquinoxaline (DPQ) unit in D-A type polymers can enhance the PCE of the PSC [26]. These results clearly demonstrate the usefulness of multiple electron-withdrawing moieties on the Qx unit for improving the photovoltaic properties of Qx-based D-A type polymers. However, additional studies focused on the effect of electron-donating moieties on various properties of these Qx-based polymers, are required for the further development of high-performance PSCs.

In this study, two Qx-based D-A type conjugated polymers with multiple electron-withdrawing groups were synthesized by Stille coupling reacation. Indacenodithiophene (IDT) and indacenodithieno[3,2-b]thiophene (IDTT) were selected as the D units, because their rigid coplanar structures are beneficial for facilitating charge transfer and charge transport in PSCs [27,28]. In addition, as mentioned, the DPQ derivative named as $DPQCF_3F$, in which two CF_3 and two F units are incorporated into the *meta*-positions of the phenyl substituents on the 2,3-positions of DPQ and the 6,7-positions of DPQ, respectively, was used as the A component [24]. The combination of IDT and IDTT with $DPQCF_3F$ through a thiophene bridge produced **PIDT-Qx** and **PIDTT-Qx**, respectively (Fig. 1). To investigate the photovoltaic properties of the polymers, an inverted-type PSC with the structure of indium tin oxide (ITO)/ZnO/active layer(polymer:$PC_{71}BM$)/MoO_3/Ag was fabricated. Owing to the significant contribution of the $DPQCF_3F$ unit in the polymer backbone, V_{oc} of the device is increased up to 0.92 V. Furthermore, the PSC based on **PIDTT-Qx** exhibited a higher PCE of 4.54% than that of the PSC based on **PIDT-Qx** (2.83%). The enhanced light absorption and charge-carrier mobility of **PIDTT-Qx** caused by the replacement of two thiophene rings in IDT by two thieno[3,2-b]thiophene units in IDTT could be attributed to this improvement in the PSCs.

Experimental

Syntheses

Synthesis of PIDT-Qx

In a Schlenk flask, the 1,1′-[4,4,9,9-tetrakis(4-hexylphenyl)-4,9-dihydro-s-indaceno[1,2-b:5,6-b′]dithiophene-2,7-diyl]bis[1,1,1-trimethylstannane (IDT, 0.20 mmol), dibrominated quinoxaline monomer 5,8-bis(5-bromothiophen-2-yl)-2,3-bis(4-((2-ethylhexyl)oxy)-3-(trifluoromethyl)phenyl)-6,7-difluoroquinoxaline ($DPQCF_3F$, 0.20 mmol), and tetrakis(triphenylphosphine)palladium (0) (3 mol%) were mixed together in 10 mL of anhydrous toluene. The solution was degassed using nitrogen for 15 min and then stirred at 90 °C under a nitrogen atmosphere for 48 h. After polymerization, the end-capping agents (2-trimethylstannylthiophene and 2-bromothiophene) were added one by one at a 2 h interval. After cooling to room temperautre, the reaction mixture was precipitated into methanol and the solids were collected by filtration. Soxhlet extraction with methanol, acetone, hexane, and chloroform was conducted for further purification. The final solution in a chloroform fraction was concentrated and precipitated into methanol. Finally, the polymer was dried overnight at 50 °C under a vacuum condition. Yield = 89%. ^{1}H NMR (400 MHz, $CDCl_3$): δ (ppm) = 8.35–8.25 (m, 2H), 8.05–7.96 (m, 2H), 7.72 (s, 2H), 7.46–7.37 (br, 2H), 7.34–7.29 (br, 2H), 7.25–7.16 (br, 8H), 7.12–7.03 (br, 10H), 6.99–6.91 (br, 2H), 4.03–3.90 (br, 4H), 2.61–2.52 (br, 8H), 1.82–1.73 (br, 2H), 1.59–1.22 (m, 48H), 0.95–0.86 (m, 24H). Molecular weight by GPC: number-average molecular weight (M_n) = 25.18 KDa, polydispersity index (PDI) = 1.78. Elemental analysis: calcd (%) for $C_{110}H_{118}F_8N_2O_2S_4$: C 74.21, H 6.68, N 1.57, S 7.20; found: C 73.49, H 6.58, N 1.33, S 7.31.

Synthesis of PIDTT-Qx

PIDTT-Qx was prepared using the same method as explained above. The Stille coupling reaction between 1,1′-[6,6,12,12-tetrakis (4-hexylphenyl)-6,12-dihydrodithieno[2,3-d:2′,3′-d′]-s-indaceno [1,2-b:5,6-b′]dithiophene-2,8-diyl]bis[1,1,1-trimethylstannane] (IDTT, 0.20 mmol) and dibrominated quinoxaline monomer ($DPQCF_3F$, 0.20 mmol) was conducted. Yield = 85%. ^{1}H NMR (400 MHz, $CDCl_3$): δ (ppm) = 8.45–8.38 (m, 2H), 8.06–7.95 (m, 2H), 7.72–7.61 (m, 2H), 7 .56–7.50 (m, 4H), 7.37–7.34 (m, 2H), 7.26–7.16 (m, 8H), 7.14–7.08 (m, 8H), 7.01–6.95 (br, 2H), 4.05–3.95 (br, 4H), 2.62–2.52 (br, 8H), 1.83–1.78 (br, 2H), 1.60–1.22 (m, 48H), 0.98–0.86 (m, 24H). Molecular weight by GPC: M_n = 33.15 KDa, PDI = 2.22. Elemental analysis: calcd (%) for $C_{114}H_{118}F_8N_2O_2S_8$: C 72.35, H 6.28, N 1.48, S 10.17; found: C 71.66, H 6.17, N 1.25, S 10.57.

Results and discussion

Synthesis and thermal properties of the polymers

As shown in Scheme 1, two Qx-based conjugated polymers with a D-A structure were synthesized by the Stille coupling reaction. The electron-donating IDT and IDTT moieties were linked with the electron-accepting $DPQCF_3F$ through a thiophene bridge to yield **PIDT-Qx** and **PIDTT-Qx**, respectively. Owing to the presence of alkyl and alkoxy chains on the IDT and IDTT donors, and $DPQCF_3F$ acceptor, respectively, **PIDT-Qx** and **PIDTT-Qx** exhibited good solubility in common organic solvents such as chloroform, tetrahydrofuran, and toluene. As measured by GPC, the average molecular weights of **PIDT-Qx** and **PIDTT-Qx** were 25.18 and 33.15 KDa with polydispersity indexes of 1.78 and 2.22, respectively. In addition, according to the thermogravimetric analysis (TGA) conducted at a heating rate of 10 °C/min under a nitrogen atmosphere, **PIDT-Qx** and **PIDTT-Qx** displayed excellent thermal

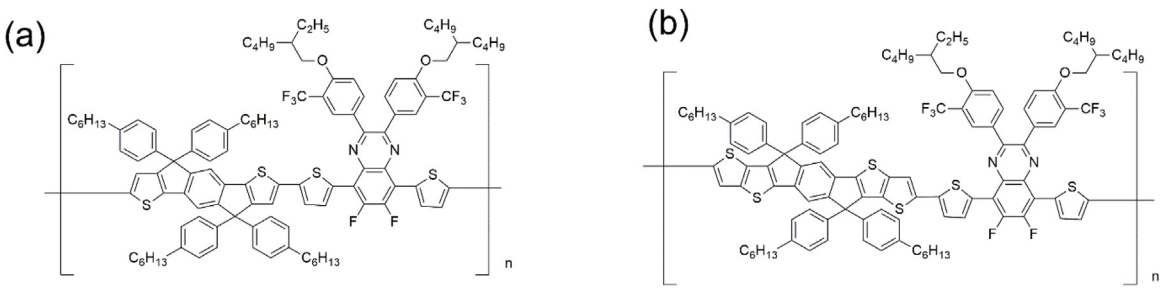

Fig. 1. Chemical structures of (a) **PIDT-Qx** and (b) **PIDTT-Qx**.

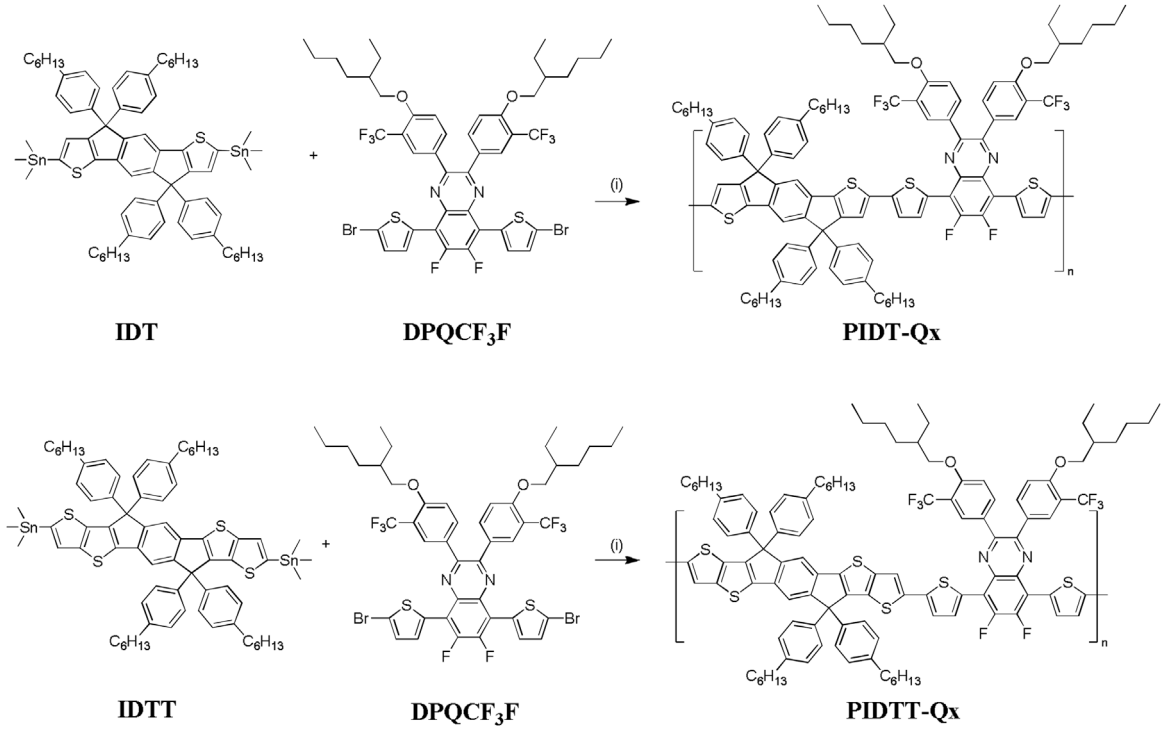

Scheme 1. Synthesis of **PIDT-Qx** and **PIDTT-Qx**. (i) $Pd(PPh_3)_4$, toluene, 90 °C, and 48 h.

stability with approximately the same high onset decomposition temperature of 420 °C at a 5 wt% loss ($T_{d5\%}$) (Fig. 2).

Optical and electrochemical properties

As expected from the typical D-A structure, the UV-visible spectra of **PIDT-Qx** and **PIDTT-Qx** in the films exhibited two broad absorption peaks in the shorter (350–500 nm) and longer (500–650 nm) wavelength regions (Fig. 3a). The former is responsible for the localized π–π* transition of the polymer backbones, while the latter indicates the existence of intramolecular charge transfer (ICT) between the IDT or IDTT donors and the $DPQCF_3F$ acceptor. While the absorption peaks of **PIDT-Qx** and **PIDTT-Qx** in the longer wavelength were located at approximately the same position (~590 nm), the shorter wavelength peak of the **PIDTT-Qx** (462 nm) was slightly red-shifted compared to that of **PIDT-Qx** (450 nm) because of the more extended conjugation length of the IDTT donor than that of IDT. In addition, the same optical bandgap of 1.75 eV was monitored from UV–vis spectra of the polymer films. However, the molar absorption coefficient (ε) of **PIDTT-Qx** at the absorption maximum wavelength was higher than that of **PIDT-Qx** in the solution phase owing to the stronger ICT formation between IDTT and $DPQCF_3F$ in **PIDTT-Qx** (Table 1). This result agrees well with previous results [29].

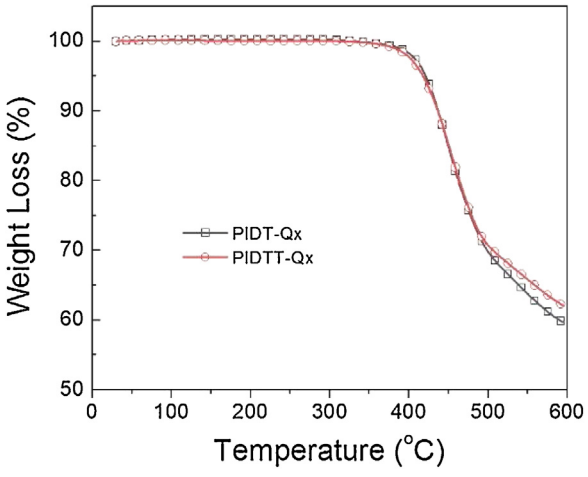

Fig. 2. TGA thermograms of **PIDT-Qx** and **PIDTT-Qx**.

CV measurements were also conducted to investigate the electrochemical properties of the polymers. The HOMO energy levels of **PIDT-Qx** and **PIDTT-Qx** calculated from the onset oxidation potential in the CV curves with a ferrocene/ferrocenium standard were −5.21 and −5.27 eV, respectively. Meanwhile, the LUMO energy levels obtained from the HOMO level and the optical bandgap were −3.30 and −3.36 eV, respectively. Therefore, the HOMO and LUMO energy level were slightly lowered by the replacement of the two thiophene rings in **PIDT-Qx** by the two thieno[3,2-b]thiophene units in **PIDTT-Qx**. Similar trends in the energy levels of the IDT and IDTT-based D-A type polymers were observed from a previous report [28]. Furthermore, the energy level diagrams of **PIDT-Qx**, **PIDTT-Qx**, and other materials used in this study are shown in Fig. S1 in the electronic supporting information (ESI). A favorable photo-induced charge generation and transport process were demonstrated in the inverted-type PSCs. The optical and electrochemical properties of **PIDT-Qx** and **PIDTT-Qx** are listed in Table 1.

Theoretical calculation

The density functional theory at the B3LYP/6-31G** level of the Gaussian 09 program was utilized to determine the distribution of the frontier molecular orbitals of **PIDT-Qx** and **PIDTT-Qx** [30]. For the simple calculation, all the alkyl and alkoxy chains in the IDT or IDTT donors and $DPQCF_3F$ acceptor were abbreviated to methyl and

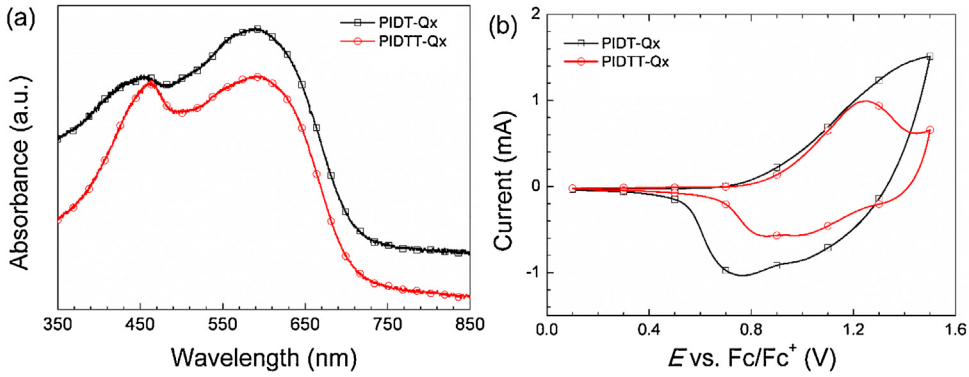

Fig. 3. (a) UV-visible spectra of the polymers films on the glass substrate (film spectra are offset for clarity) and (b) cyclic voltammograms of **PIDT-Qx** and **PIDTT-Qx**.

Table 1
Summary of the optical and electrochemical properties of the polymers.

Polymer	λ_{edge}(nm)[a] E_{gap}^{opt}(eV)[b]	$\lambda_{max}^{solution}$ (nm)[c] (λ_{max}^{film} (nm)[d])	ε ($M^{-1}\,cm^{-1}$)[e]	HOMO (eV)[f]	LUMO (eV)[g]
PIDT-Qx	708, 1.75	455, 572 (450, 589)	4.26×10^4	−5.21	−3.30
PIDTT-Qx	707. 1.75	460, 572 (462, 589)	4.62×10^4	−5.27	−3.36

[a] Absorption edge of the polymer film.
[b] Optical band gap estimated from the absorption edge.
[c] Maximum absorption wavelength of the polymer solution in chlorobenzene.
[d] Maximum absorption wavelength of the film.
[e] Molar extinction coefficient of the polymer solution in chlorobenzene.
[f] Estimated from the oxidation onset potential.
[g] Calculated from the optical band gap and the HOMO energy level.

methoxy groups, respectively. Similarly, the long polymer backbones were reduced to two repeating units and used for the computational calculation. As shown in Fig. 4, the HOMO wave functions in the two repeating units of **PIDT-Qx** and **PIDTT-Qx** were generally delocalized along the whole chains, while the LUMO wave functions were mostly localized over the electron-withdrawing $DPQCF_3F$ unit. In addition, the theoretical HOMO/LUMO energy levels for **PIDT-Qx** and **PIDTT-Qx** were −4.55/-2.50 eV and −4.56/−2.54 eV, respectively. This is in agreement in UV-visible and CV measurements (*vide supra*).

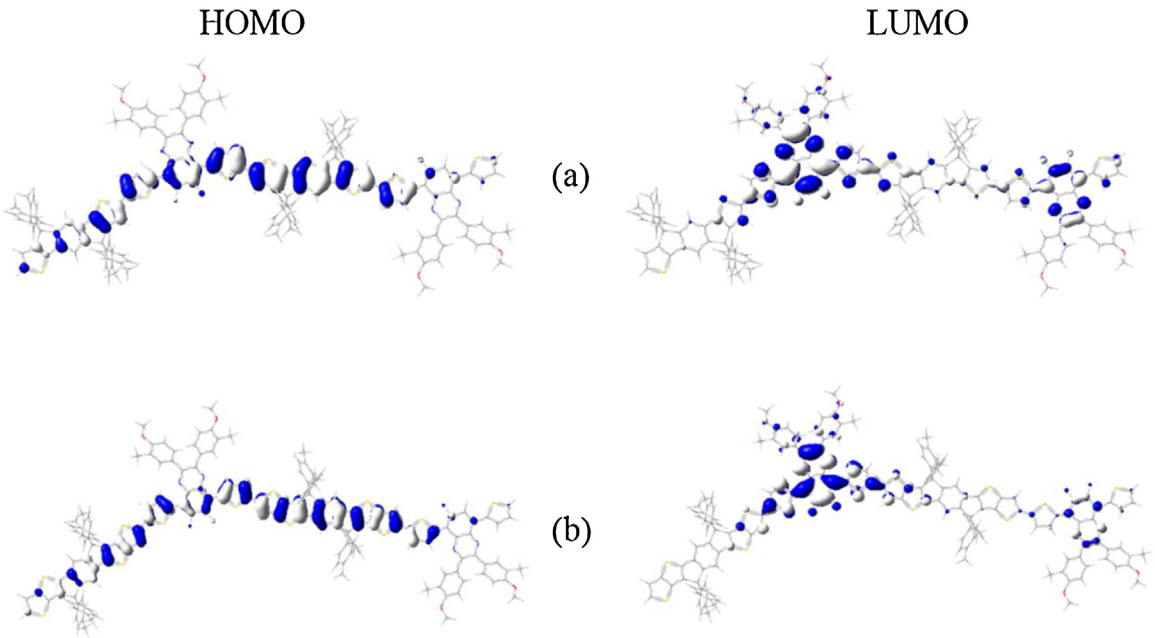

Fig. 4. Frontier molecular orbitals of two-repeating unit models calculated by the B3LYP/6-31G** level for (a) **PIDT-Qx** and (b) **PIDTT-Qx**.

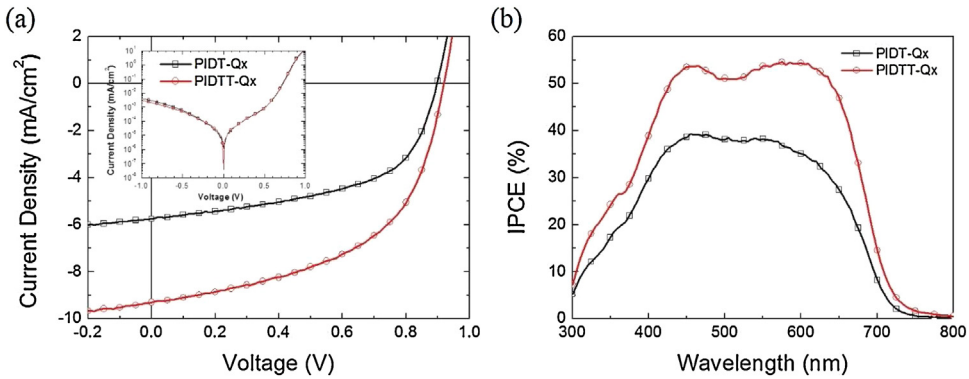

Fig. 5. (a) Current density vs. voltage curves of the PSCs under a 1.0 sun condition (inset: under the dark condition) and (b) the IPCE spectra of the PSCs based on **PIDT-Qx** and **PIDTT-Qx**.

Table 2
Summary of the best photovoltaic parameters of the PSCs. The average values of the parameters of each device are given in parentheses.

Polymer	J_{sc} (mA/cm^2)	V_{oc} (V)	FF (%)	PCE (%)	R_s (Ω cm^2)[a]
PIDT-Qx	5.75 (5.63 ± 0.07)	0.90 (0.90 ± 0.00)	54.6 (55.2 ± 0.36)	2.83 (2.80 ± 0.04)	5.72
PIDTT-Qx	9.30 (9.16 ± 0.09)	0.92 (0.92 ± 0.00)	53.0 (53.1 ± 0.21)	4.54 (4.48 ± 0.04)	4.60

[a] Series resistance is estimated from the corresponding best device.

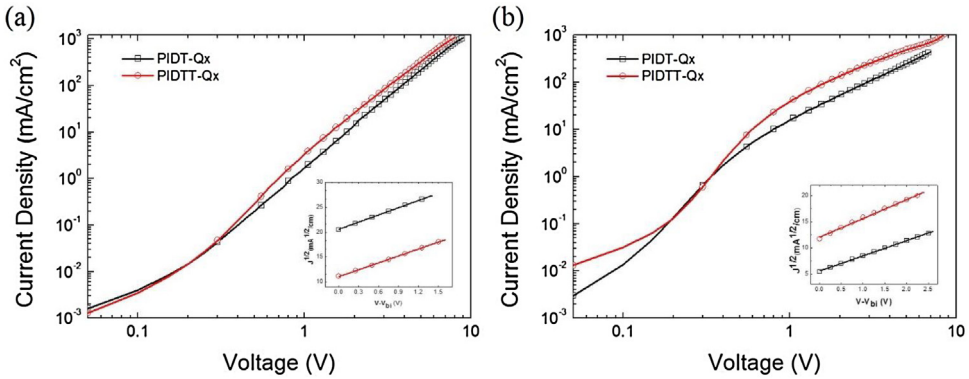

Fig. 6. Current density vs. voltage curves of (a) the electron- and (b) hole-only devices (inset: current density vs. voltage (V)-built-in voltage (V_{bi}) curves with the fitted line) based on **PIDT-Qx** and **PIDTT-Qx**.

Photovoltaic properties

The photovoltaic performances of **PIDT-Qx** and **PIDTT-Qx** were investigated by fabricating the inverted-type PSC with the ITO/ZnO/active layer(polymer:$PC_{71}BM$)/MoO_3/Ag structure. During the preparation of the active layers, 1,8-diiodooctane (DIO) was utilized as a processing additive. After testing the photovoltaic performance of the device using several blend ratios of the polymer and $PC_{71}BM$ in the active layer ranging from 3:3 to 3:12 w/w (Table S1 in ESI), the optimal blend ratios for **PIDT-Qx** and **PIDTT-Qx** were determined to be 3:6 and 3:4, respectively. Fig. 5a shows the current density-voltage (*J-V*) curves of the PSCs with the optimum blend ratios under AM 1.5G simulated illumination. The PCE of the PSC with **PIDT-Qx** was limited to 2.83%, while that of the device based on **PIDTT-Qx** was significantly improved to 4.54%. This profound enhancement in the PCEs of the device with **PIDTT-Qx** was attributed to its higher short circuit current (J_{sc}) of 9.50 mA/cm^2 than that of the device with **PIDT-Qx** (5.75 mA/cm^2) (Fig. 5a). Meanwhile, similar values of the open-circuit voltage (V_{oc}) near 0.90 V as well as the fill factor (*FF*) of approximately 53–55% were observed from both PSCs with **PIDT-Qx** and **PIDTT-Qx** (Table 2). The strong electron-withdrawing $DPQCF_3F$ moiety in **PIDT-Qx** and **PIDTT-Qx** increased V_{oc} of the devices up to 0.92 V, which is comparable to other polyquinoxaline-based PSCs with the similar multiple electron-withdrawing units [25,31]. In addition, the series resistance (R_s) was calculated from the *J-V* curves of the PSC under a dark condition (inset of Fig. 5a). The R_s of the device with **PIDTT-Qx** (4.60 Ω cm^2) was smaller than that of the device adopting **PIDT-Qx** (5.72 Ω cm^2), which was consistent with the photovoltaic performances of the PSCs. Furthermore, the incident photon-to-current efficiency (IPCE) was measured, and the data are shown in Fig. 5b. The PSCs based on **PIDT-Qx** and **PIDTT-Qx** exhibited good responses from 300 to 800 nm, and the higher efficiency was monitored from the device with **PIDTT-Qx**. All IPCE spectra agreed well with the J_{sc} values of the devices.

The charge transporting properties of the polymers were also investigated by constructing hole-only and electron-only devices. As shown in Fig. 6a and b , the *J-V* curves of both devices exhibited the featured behavior of the space charge limited current (SCLC) and were governed by the well-known Mott–Gurney law [32]. Although, there is no significant difference in the electron mobility of both polymers-based device, the hole mobility of the device with **PIDTT-Qx** (1.30×10^{-3} cm^2 V^{-1} s^{-1}) was higher than that of the **PIDT-Qx** based device (8.89×10^{-4} cm^2 V^{-1} s^{-1}). Furthermore,

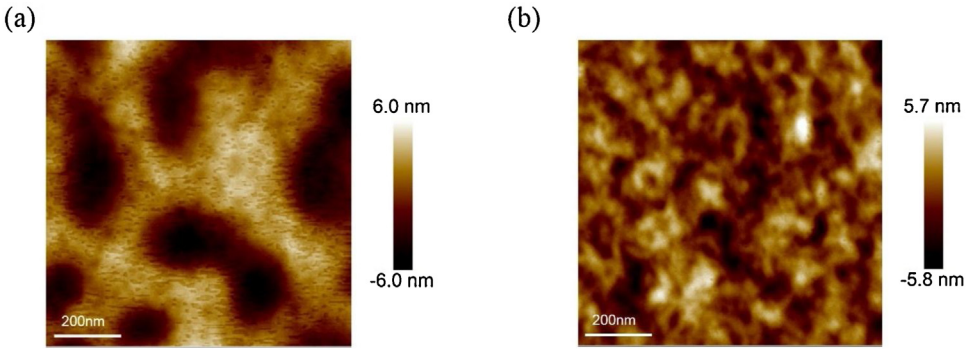

Fig. 7. AFM images of the surface of (a) **PIDT-Qx**:$PC_{71}BM$, and (b) **PIDTT-Qx**:$PC_{71}BM$.

the ratio of the electron and hole mobility of the device based on **PIDTT-Qx** (0.96) was more balanced than that of the device based on **PIDT-Qx** (1.54). These results supported the higher J_{sc} value of the photovoltaic cell with **PIDTT-Qx** compared to that of the device with **PIDT-Qx**.

The surface morphology of the active layer of the photovoltaic cells was examined by the tapping-mode atomic force microscopy (AFM) measurements, and the results are shown in Fig. 7. The root-mean-squares (RMSs) of the surface of the active layer based on **PIDT-Qx** and **PIDTT-Qx** were 3.46 nm and 1.51 nm, respectively, which demonstrated a more favorable nanoscale phase separation in the blended film of **PIDTT-Qx** and $PC_{71}BM$. This smoother surface of the active layer of the **PIDTT-Qx** based device could also contribute to its higher value of J_{sc} than that of the device with **PIDT-Qx** through a more efficient charge separation and transport.

Conclusion

Two quinoxaline-based conjugated polymers with a typycal donor-π-acceptor structure were synthesized by the Stille coupling reacation. The electron-donating IDT and IDTT derivatives were connected to the electron-withdrawing $DPQCF_3F$ that contained multiple CF_3 and F moieties through a thiophene bridge to produce **PIDT-Qx** and **PIDTT-Qx**, respectively. To investigate the photovoltaic properties of the two polymers, the inverted-type PSC with the ITO/ZnO/active layer(polymer:$PC_{71}BM$)/MoO_3/Ag structure was fabricated and tested. Owing to the significant contribution of the $DPQCF_3F$ unit in the polymer backbones, V_{oc} of the related PSCs are increased up to 0.92 V. In addition, a higher PCE of 4.54% was observed from the device with **PIDTT-Qx** than that of the device based on **PIDT-Qx** (2.83%), owing to the significant enhancement in J_{sc} from 5.75 mA/cm^2 for the device with **PIDT-Qx** to 9.50 mA/cm^2 for the device with **PIDTT-Qx**. The replacement of the thiophene units in IDT by the thieno[3,2-b] thiophene groups in IDTT improved the light absorption and charge carrier mobility of **PIDTT-Qx**, and thereby, the J_{sc} value of the PSC based on **PIDTT-Qx** was enhanced. Therefore, this study provides meaningful information for the logical design and structure-property relationships of donor-acceptor type polymers with multiple electron-withdrawing substituents for photovoltaic applications.

Acknowledgement

This research was supported by Basic Science Researches through the National Research Foundation (NRF) of Korea under program number (2018R1D1A1B07042822) and Korea Institute of Energy Technology Evaluation and Planning (KETEP-2018201010636),

Appendix A. Supplementary data

Supplementary data associated with this article can be found, in the online version, at https://doi.org/10.1016/j.jiec.2019.01.024.

References

[1] Y.-J. Cheng, S.-H. Yang, C.-S. Hsu, Chem. Rev. 109 (2009) 5868.
[2] G. Li, R. Zhu, Y. Yang, Nat. Photonics. 6 (2012) 153.
[3] S. Günes, H. Neugebauer, N.S. Sariciftci, Chem. Rev. 107 (2007) 1324.
[4] J. Zhang, W. Cai, F. Huang, E. Wang, C. Zhong, S. Liu, M. Wang, C. Duan, T. Yang, Y. Cao, Macromolecules 44 (2011) 894.
[5] G. Dennler, M.C. Scharber, C.J. Brabec, Adv. Mater. 21 (2009) 1323.
[6] P.W.M. Blom, V.D. Mihailetchi, L.J.A. Koster, D.E. Markov, Adv. Mater. 19 (2007) 1551.
[7] S. Li, L. Ye, W. Zhao, S. Zhang, S. Mukherjee, H. Ade, J. Hou, Adv. Mater. 28 (2016) 9423.
[8] W. Zhao, S. Li, H. Yao, S. Zhang, Y. Zhang, B. Yang, J. Hou, J. Am. Chem. Soc. 139 (2017) 7148.
[9] D. He, F. Zhao, J. Xin, J.J. Rech, Z. Wei, W. Ma, W. You, B. Li, L. Jiang, Y. Li, C. Wang, Adv. Energy Mater. 8 (2018)1802050, doi:http://dx.doi.org/10.1002/aenm.201802050.
[10] Y. Zhu, R.D. Champion, S.A. Jenekhe, Macromolecules 39 (2006) 8712.
[11] J.S. Wu, Y.J. Cheng, M. Dubosc, C.H. Hsieh, C.Y. Chang, C.S. Hsu, Chem. Commun. 46 (2010) 3259.
[12] S.J. Nam, S.J. Jeon, Y.W. Han, D.K. Moon, J. Ind. Eng. Chem. 63 (2018) 191.
[13] Y. Eom, C.E. Song, W.S. Shin, S.K. Lee, E. Lim, J. Ind. Chem. Eng. 45 (2017) 338.
[14] A.C. Stuart, J.R. Tumbleston, H. Zhou, W. Li, S. Liu, H. Ade, W. You, J. Am. Chem. Soc. 135 (2013) 1806.
[15] S.C. Price, A.C. Stuart, L. Yang, H. Zhou, W. You, J. Am. Chem. Soc. 133 (2011) 4625.
[16] X.P. Xu, Y. Li, M.M. Luo, Q. Peng, Chinese Chem. Lett. 27 (2016) 1241.
[17] A. Casey, S.D. Dimitrov, P. Shakya-Tuladhar, Z. Fei, M. Nguyen, Y. Han, T.D. Anthopoulos, J.R. Durrant, M. Heeney, Chem. Mater. 28 (2016) 5110.
[18] Y. Huang, L. Huo, S. Zhang, X. Guo, C.C. Han, Y. Li, J. Hou, Chem. Commun. 47 (2011) 8904.
[19] J.Y. Shim, T. Kim, J. Kim, J. Kim, I. Kim, J.Y. Kim, H. Suh, Synth. Met. 205 (2015) 112.
[20] Y. Lu, Z. Xiao, Y. Yuan, H. Wu, Z. An, Y. Hou, C. Gao, J. Huang, J. Mater. Chem. C 1 (2013) 630.
[21] H.J. Jhuo, P.N. Yeh, S.H. Liao, Y.L. Li, Y.S. Cheng, S.A. Chen, J. Chinese Chem. Soc. 61 (2014) 115.
[22] C.P. Chen, Y.C. Chen, C.Y. Yu, Polym. Chem. 4 (2013) 1161.
[23] D. Liu, W. Zhao, S. Zhang, L. Ye, Z. Zheng, Y. Cui, Y. Chen, J. Hou, Macromolecules 48 (2015) 5172.
[24] P. Yang, M. Yuan, D.F. Zeigler, S.E. Watkins, J.A. Lee, C.K. Luscombe, J. Mater. Chem. C 2 (2014) 3278.
[25] S.K. Putri, Y.H. Kim, D.R. Whang, M.S. Lee, J.H. Kim, D.W. Chang, Org. Electron. 47 (2017) 14.
[26] S.K. Putri, Y.H. Kim, D.R. Whang, J.H. Kim, D.W. Chang, Macromol. Rapid Commun. 39 (2018)1800260.
[27] Y. Zhang, J. Zou, H.L. Yip, K.S. Chen, D.F. Zeigler, Y. Sun, A.K.Y. Jen, Chem. Mater. 23 (2011) 2289.
[28] Y. Cai, X. Zhang, X. Xue, D. Wei, L. Huo, Y. Sun, J. Mater. Chem. C 5 (2017) 7777.
[29] Y.X. Xu, C.C. Chueh, H.L. Yip, F.Z. Ding, Y.X. Li, C.Z. Li, X. Li, W.C. Chen, A.K.Y. Jen, Adv. Mater. 24 (2012) 6356.
[30] M.J. Frisch, G. Trucks, H.B. Schlegel, G. Scuseria, M. Robb, J. Cheeseman, G. Scalmani, V. Barone, B. Mennucci, G. Petersson, Gaussian 09, Revision A. 1, Gaussian Inc., Wallingford, CT, 2009, pp. 34.
[31] J. Yuan, L. Qiu, Z. Zhang, Y. Li, Y. He, L. Jiang, Y. Zou, Chem. Commun. 52 (2016) 6881.
[32] A. Bagui, S.S.K. Iyer, Org. Electron. Phys. Mater. Appl. 15 (2014) 1387.